

Supplemental materials 1: MIFlowCyt-EV of clinical research study “Ticagrelor attenuates the increase of extracellular vesicles concentrations in plasma after acute myocardial infarction compared to clopidogrel”

1 Flow cytometry

1.1 Experimental design

The aim of flow cytometry (A60-Micro, Apogee Flow Systems, Hemel Hempstead, UK) was to compare the concentrations of extracellular vesicles (EVs) released from activated platelets (CD61⁺/P-selectin⁺ or fibrinogen⁺), leukocytes (CD45⁺), ECs (CD31⁺/CD146⁺) and all procoagulant EVs (PS⁺) in platelet free plasma (PFP) between 30 patients treated with ticagrelor and 30 patients treated with clopidogrel after first acute myocardial infarction (AMI). We hypothesized that 6 months after first AMI, patients treated with ticagrelor have a significantly lower concentration of activated platelet EVs, leukocyte EVs, endothelial cell (EC) EVs, and procoagulant EVs in PFP compared to patients treated with clopidogrel. As a control, we measured the concentration of EVs from erythrocytes (CD235a⁺). Since erythrocytes do not expose P2Y12 receptors [1], we expected no significant differences in the concentration of erythrocyte EVs between the study groups. Pre-analytical variables can be found in the manuscript.

All samples were measured using an autosampler, which facilitates subsequent measurements of samples in a 96-well plate. The entire study involved fifteen 96-well plates that were measured within 5 months during three periods of 7 subsequent days, 2 subsequent days and 1 day. Each well plate contained a buffer-only control. In addition, each well plate contained the antibody in buffer controls and isotype controls corresponding to the labels in the well plate. Scatter calibrations were performed daily. Fluorescence calibration and flow rate calibration were performed once. To automatically determine optimal samples dilutions, apply calibrations, determine and apply gates, generate reports with scatter plots and generate data summaries, we developed and applied custom-build software (MATLAB R2018b, Mathworks, Natick, MA, USA).

1.2 Sample dilutions

Because the particle concentration in PFP differs between individuals, samples require different dilutions to avoid swarm detection [2] and to achieve statistically significant counts within a clinically applicable measurement time. Although serial dilutions are recommended to find the optimal dilution, we consider serial dilutions unfeasible in a study with 60 donors and 3 time points. Therefore, we developed a procedure to estimate to optimal sample dilution (Section 1.2 of <https://doi.org/10.6084/m9.figshare.c.4753676.v1>). In sum, we showed that for our flow cytometer and settings used, a count rate $\leq 5.0 \cdot 10^3$ events second unlikely results in swarm detection.

To find the dilution resulting in a count rate $\leq 5.0 \cdot 10^3$ events per second, we diluted each PFP sample 2,000-fold in phosphate buffered saline (PBS) and measured the total concentration of particles for 30 seconds without staining. For all experiments, PBS was filtered (Whatman 50 nm, Sigma-Aldrich, US) and had a pH of 7.4. By diluting each sample 2,000-fold, all but 2 samples had a count rate $\leq 5.0 \cdot 10^3$ events per second. Figure S1A shows a distribution of the measured total particle concentrations of all samples in the study. Taking into account the measured concentration and flow rate, we calculated the minimum pre-dilution required before staining (next section) to achieve a count rate $\leq 5.0 \cdot 10^3$ events per second after staining. The staining procedure adds an extra dilution of 11.1-fold to the overall dilution. To simplify procedures, samples were divided into 7 categories of pre-dilution: 10-fold, 20-fold, 40-fold, 80-fold, 200-fold, 250-fold and 400-fold. Figure S1B shows a distribution of the applied pre-dilutions of all samples in the study.

1.3 EV staining

EVs in PFP were stained with antibodies and lactadherin. Prior to staining, antibodies were diluted in PBS and centrifuged at 18,890 g for 5 min to remove aggregates. Table S1 shows an overview of the used reagents and antibody concentrations during staining. Each sample was double labelled with CD31-APC (allophycocyanin) and CD146-PE (phycoerythrin), with CD45-APC and Lac-FITC (fluorescein isothiocyanate), with CD61-APC and CD62p-PE, with CD61-APC and Fib-FITC, and single labelled with CD235-PE. To stain, 20 μL of pre-diluted (Figure S1B) PFP was incubated with 2.5 μL of antibodies or isotype controls and kept in the dark for 2 h at room temperature. The staining reaction was stopped by adding 200 μL of citrated (0.32%) PBS.

1.4 Buffer-only control

Each 96-wellplate contained at least 1 well with filtered (Whatman 50 nm) PBS, which was measured with the same flow cytometer and acquisition settings as all other samples. The mean count rate was 98.4 events per second, which is substantially lower than the target count rate ($2.5\text{-}5.0 \cdot 10^3$ events per second) for PFP samples. A summary of the buffer-only control can be found in the compressed data summary files

(<https://www.doi.org/10.6084/m9.figshare.11340386>, Control_buffer-only_flow_rate.pdf and Control_buffer-only_scatter_plots.pdf).

1.5 Buffer with reagents control

Each 96-wellplate contained a buffer with reagent control for each reagent (Table S1), which was measured with the same flow cytometer and acquisition settings as all other samples. For all reagents but CD61-APC, the mean count rate was 87.6 events per second, which is similar to the buffer-only control. CD61-APC in buffer resulted in a count rate of 931.3 events per second, which is substantially higher than the buffer-only control. To investigate how the relatively high counts in CD61-APC in buffer affect the sample measurements, we applied the same calibrations and gates to CD61-APC in buffer as to the PFP samples stained with CD61-APC. For particles with a diameter >200 nm and a refractive index <1.42 , as reported in this study, we measured under the same conditions on average 1.8 CD61-APC+ events per second in buffer compared to 42.8 CD61-APC+ events per second in PFP. Here, we omitted measurement CD61-APC_C1_0, which was an outlier with 37.6 CD61-APC+ events per second. We conclude that the count rate of CD61-APC in buffer, which is high compared to the count rate of the buffer-only control, is negligible (4%) compared to the count rate of CD61-APC+ events in PFP. A summary of the buffer with reagents control can be found in the compressed data summary files (<https://www.doi.org/10.6084/m9.figshare.11340386>, Control_buffer_with_reagents_flow_rate.pdf, Control_buffer_with_reagents_scatter_plots.pdf, Control_buffer-only_CD61-APC_flow_rate.pdf, and Control_buffer-only_CD61-APC_gates.pdf).

1.6 Unstained controls

Unstained controls were measured at 2,000-fold, which differs from the dilution with which the stained PFP samples were measured. Whether 2,000-fold diluted samples are a useful unstained control requires further investigation.

1.7 Isotype controls

Table S1 shows an overview of the used isotype controls. For particles with a diameter >200 nm and a refractive index <1.42, as reported in this study, we measured on average 0.0 APC+ events per second for IgG-APC, 0.2 FITC+ events per second for PolyG-FITC, and 0.0 PE+ events per second for IgG-PE. Here, we omitted measurement PolyG-FITC_C11_0, which was an outlier with 10.2 CD61-APC+ events per second.

1.8 Trigger channel and threshold

Based on the buffer-only control (98.4 events s⁻¹), the acquisition software was set up to trigger at 14 arbitrary units SSC, which is equivalent to a side scattering cross section of 10 nm² (Rosetta Calibration, v1.11, Exometry, Amsterdam, The Netherlands).

1.9 Flow rate quantification

We used concentration reference particles (TruCount, BD Biosciences, Franklin Lakes, NJ, USA) to calibrate the flow rate of a needle aspirated flow cytometer (FACSCalibur, BD Biosciences). With the calibrated FACSCalibur, we determined the concentration of the 380 nm fluorescent polystyrene beads in the Rosetta Calibration beads mixture. In turn, we used the 380 nm fluorescent polystyrene beads to cross calibrate the flow rate of the A60-Micro. Figure S2 shows the measured flow rate at the A60-Micro versus the date that experiments were performed. The adjusted flow rate is 3.01 μL/min and the measured median flow rate is 2.83 μL/min. For all days except 2018-12-30, the measured flow rate was within 14% of the adjusted flow rate. Because at operational days closest to 2018-12-30 the flow rate was normal (within 8% of the adjusted flow rate), and because the A60-Micro is equipped with a syringe pump with volumetric control, we suspect that the deviation at 2018-12-30 is an artifact. To calculate EV concentrations, we assumed a flow rate of 3.01 μL/min for all measurements.

1.10 Fluorescence calibration

Calibration of the fluorescence detectors from arbitrary units (a.u.) to molecules of equivalent soluble fluorochrome (MESF) was accomplished using 2 μm Q-APC beads (2327-51, BD), Quantum FITC-5 MESF beads (FCSC555A, Bio-Rad, Hercules, CA, USA), and SPHERO Easy Calibration Fluorescent Particles (ECFP-F2-5K, Spherotech Inc., Irma Lee Circle, IL, USA).

The 2 μm Q-APC beads did not result in linear relation between the measured mean fluorescence intensity (MFI) and the specified MESF. Figure S3A shows the signals of non-

fluorescent polystyrene beads (3000 Series Nanosphere) measured at the APC detector. Because the measured signals of non-fluorescent beads can be reasonably described with Mie theory (Rosetta Calibration), we suspect that scattered light is leaking to the APC detector. Extrapolation with Mie theory shows that 2 μm polystyrene beads, which is the size of the Q-APC beads, would result in a signal of $4.42 \cdot 10^4$ a.u. at the APC detector. Figure S3B shows that subtraction of $4.42 \cdot 10^4$ a.u. from the measured MFIs does result in a linear relation between the measured MFI and specified MESF for APC.

Calibrations of the FITC and PE detectors were performed at 2018-08-19 also did not result in a linear relation between the measured MFI and the specified MESF, perhaps because the beads almost reached their expiry date. Therefore, we used an MESF calibration from 2017-09-29 and cross calibrated the fluorescence intensity using the 380 nm fluorescent polystyrene bead of Rosetta Calibration beads, resulting in a scaling factor of 0.72 for FITC and 0.71 for PE. Figure S3C and S3D show a linear relation between the measured MFI and specified MESF for FITC and PE, respectively. For each measurement, we added fluorescent intensities in MESF to the flow cytometry data files by custom-build software (MATLAB R2018a) using following equation:

$I(\text{MESF}) = 10^{a \cdot \log_{10} I(\text{a.u.}) + b}$	Equation S1
--	-------------

where I is the fluorescence intensity, and a and b are the slope and the intercept of the linear fits in figures S3B-D, respectively.

1.11 Light scatter calibration

We used Rosetta Calibration to relate scatter measured by FSC or SSC to the scattering cross section and diameter of EVs. Figure S4 shows print screens of the scatter calibrations. We modelled EVs as core-shell particles with a core refractive index of 1.38, a shell refractive index of 1.48, and a shell thickness of 4 nm. For each measurement, we added the FSC and SSC scattering cross sections and EV diameters to the flow cytometry datafiles by custom-build software (MATLAB R2018a). The SSC trigger threshold corresponds to a side scattering cross section of 10 nm^2 .

1.12 EV diameter and refractive index approximation

Flow-SR was applied to determine the size and refractive index of particles and improve specificity by enabling label-free differentiation between EVs and lipoprotein particles [3,4]. Flow-SR was performed as previously described [3,4]. Lookup tables were calculated for

diameters ranging from 10 to 1000 nm, with step sizes of 1 nm, and refractive indices from 1.35 to 1.80 with step sizes of 0.001. The diameter and refractive index of each particle was added to the .fcs file by custom-build software (MATLAB R2018a).

Because Flow-SR requires accurate measurements of both FSC and SSC, we applied Flow-SR only to particles with diameters >200 nm and fulfilling the condition:

$\text{SSC}(\text{nm}^2) > -0.7 \cdot \text{FSC}(\text{nm}^2) + 3$	Equation S2
--	-------------

1.13 MIFlowCyt checklist

The MIFlowCyt checklist is added to Table S2.

1.14 EV number concentration

The concentrations reported in the manuscript describe the number of particles (1) that exceeded the SSC threshold, corresponding to a side scattering cross section of 10 nm², (2) that were collected during time intervals, for which the count rate was within 25% of the median count rate, (3) with a diameter >200 nm as determined by Flow-SR [3], (4) fulfilling the condition of equation S2, (5) having a refractive index <1.42 to omit false positively labeled chylomicrons, and (6) are positive at the corresponding fluorescence detector(s), per mL of PFP.

1.15 Data sharing

A summary of all flow cytometry scatter plots and gates applied are available via <https://www.doi.org/10.6084/m9.figshare.11340386>. Raw data and data with standard units (40 GB) will become available via SURFfilesender upon request (e.vanderpol@amsterdamumc.nl).

2 References

- [1] Sluyter R. P2X and P2Y receptor signaling in red blood cells. *Front Mol Biosci* Frontiers; 2015; **2**: 60.
- [2] van der Pol E, van Gemert MJC, Sturk A, Nieuwland R, van Leeuwen TG. Single vs. swarm detection of microparticles and exosomes by flow cytometry. *J Thromb Haemost* 2012; **10**: 919–30.
- [3] van der Pol E, de Rond L, Coumans FAW, Gool EL, Böing AN, Sturk A, Nieuwland R, van Leeuwen TG. Absolute sizing and label-free identification of extracellular vesicles by flow cytometry. *Nanomedicine Nanotechnology, Biol Med* 2018; **14**: 801–

10.

- [4] de Rond L, Libregts SFWM, Rikkert LG, Hau CM, van der Pol E, Nieuwland R, van Leeuwen TG, Coumans FAW. Refractive index to evaluate staining specificity of extracellular vesicles by flow cytometry. *J Extracell vesicles* 2019; .

Figures

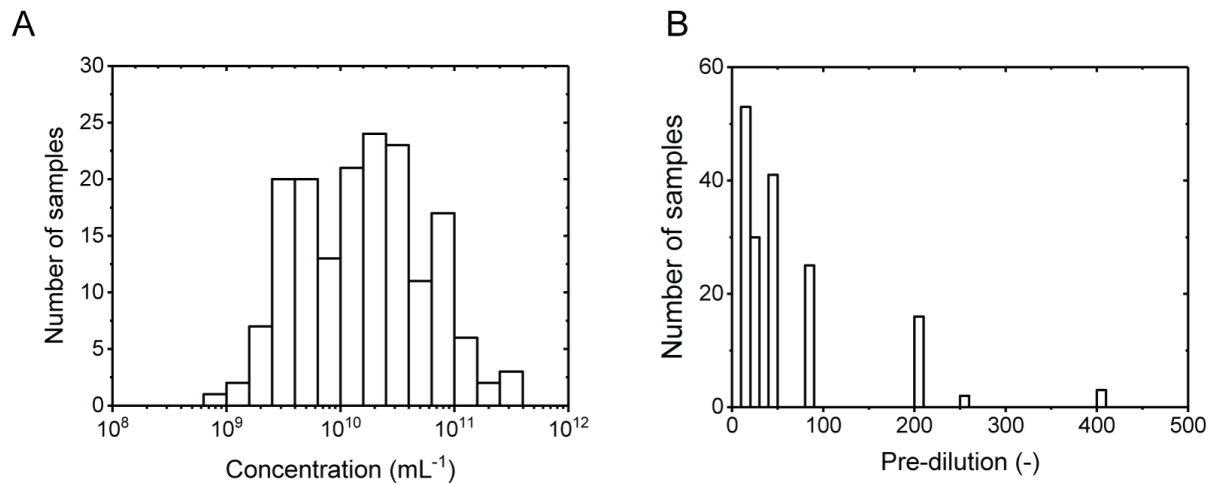


Figure S1. Distributions of (A) measured concentration of particles exceeding the side scatter threshold and (B) applied pre-dilutions of all samples in the study. The side scatter threshold corresponds to a scattering cross section of $\sim 10 \text{ nm}^2$. The measured particle concentrations differs 3 orders of magnitude, requiring pre-dilutions ranging from 10-fold to 400-fold.

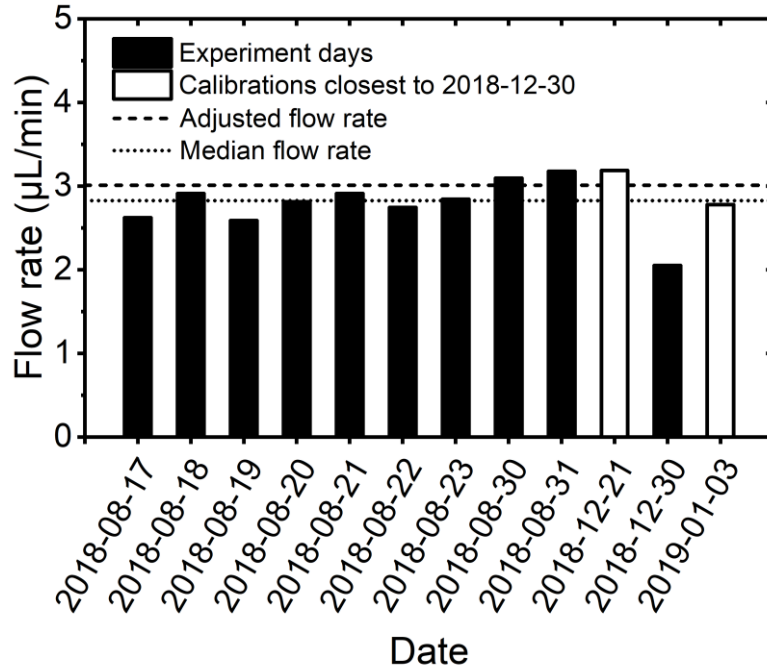


Figure S2. Measured flow rate at the A60-Micro versus date that experiments were performed. The adjusted flow rate is 3.01 µL/min and the measured median flow rate is 2.83 µL/min. For all days except 2018-12-30, the measured flow rate was within 14% of the adjusted flow rate.

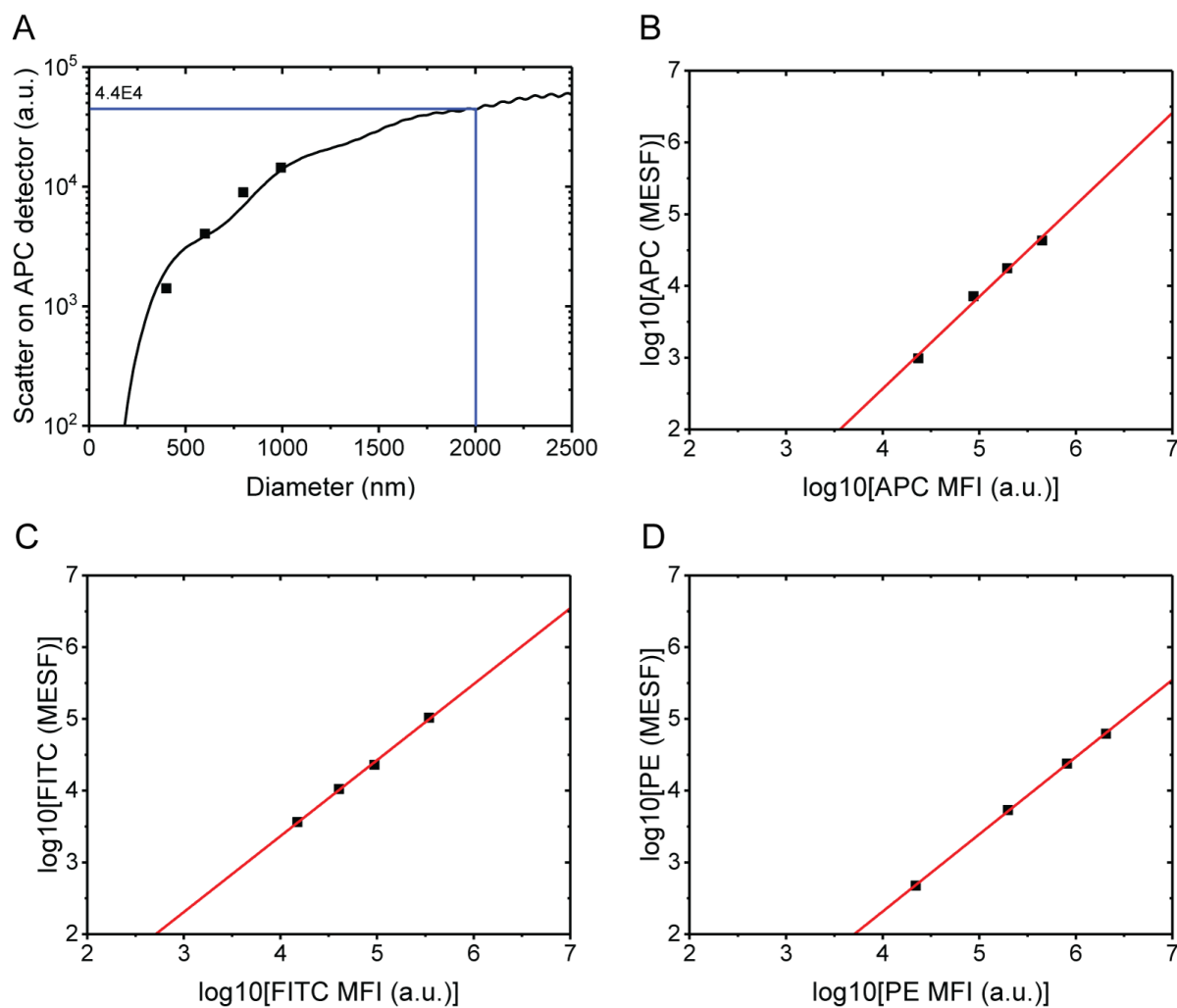


Figure S3. Calibration of the fluorescence detectors from arbitrary units (a.u.) to molecules of equivalent soluble fluorochrome (MESF). (A) Measured signals (symbols) on allophycocyanin (APC) detector of non-fluorescent polystyrene beads (3000 Series Nanosphere), suggesting a scatter leak of the spectral filter. Extrapolation with Mie theory (Rosetta Calibration) shows that 2 μm polystyrene beads leak $4.42 \cdot 10^4$ a.u. to the APC detector. Logarithmic MESF versus logarithmic mean fluorescence intensity (MFI) for (B) APC, (C) fluorescein isothiocyanate (FITC), and (D) phycoerythrin (PE). Data (symbols) are fitted with a linear function (line), resulting in a slope of 1.28 and intercept of -2.56 for APC, a slope of 1.06 and intercept of -0.87 for FITC, and a slope of 1.08 and intercept of -1.99 for PE.

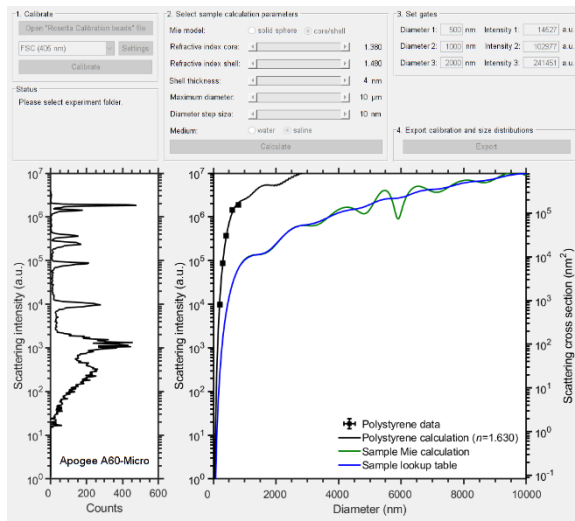
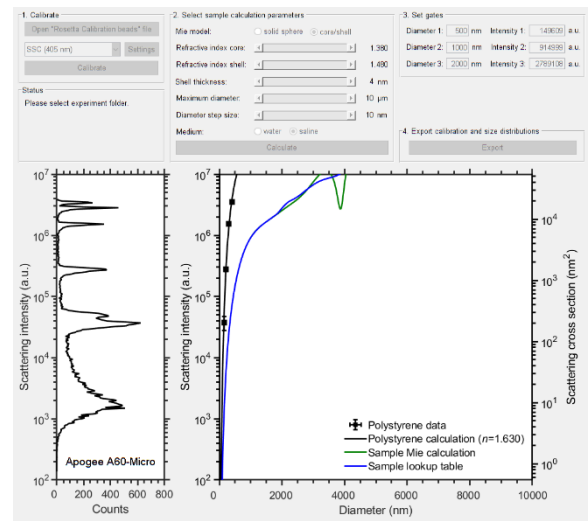
A**B**

Figure S4. Forward scatter and side scatter calibration of the A60-Micro by Rosetta

Calibration. To relate scatter to the diameter of EVs, we modelled EVs as core-shell particles with a core refractive index of 1.38, a shell refractive index of 1.48, and a shell thickness of 4 nm.

Table S1: Overview of staining reagents. Characteristics being measured, analyte, analyte detector, reporter, isotype, clone, concentration, manufacturer, catalog number and lot number of used staining reagents. The antibody concentration during measurements was 11.1-fold lower than the antibody concentration during staining.

Characteristic measured	Analyte	Analyte detector	Reporter	Isotype	Clone	Concentration during staining ($\mu\text{g mL}^{-1}$)	Manufacturer	Catalog number	Lot number
Integrin	Human CD61	Anti-human CD61 antibody	APC	IgG1	Y2/51	50	Dako	C7280	200483345
Adhesion molecule	Human CD62p	Anti-human CD62P antibody	PE	IgG1	CLB Thromb/6	6.25	Beckman Coulter	IM1759U	37
Glyco-protein	Fibrinogen	Anti-human fibrinogen antibody	FITC	Poly IgG	F0111	1700	Dako	F011102-2	20027857
Leukocyte common antigen	CD45	Anti-human CD45 antibody	APC	IgG1	2D1	25	Beckman Dickinson	340910	5040555
Glyco-protein	Lactadherin	Lactadherin	FITC	n.a.	n.a.	83	Haematologic Technologies	Blac-FITC	GG1122
Adhesion molecule	CD31	Anti-human CD31 antibody	APC	IgG1	WM59	80	Biolegend	303105	B241642
Adhesion molecule	CD146	Anti-human CD146 antibody	PE	IgG1	S-Endo 1	3.75	Biocytex	5050-PE100T	173455
Glyco-protein	CD235a	Anti-human CD235a antibody	PE	IgG1	JC159	100	Dako	R7078	20056279
Affinity for Fc receptor	Fc receptor	IgG1	APC	n.a.	X40	200	Beckman Dickinson	554681	7075605
	Fc receptor	IgG1	PE	n.a.	IS5-21F5	50	Beckman Dickinson	345816	7248665
	Fc receptor	PolyIgG	FITC	n.a.	IQP	25	Beckman Dickinson	IQP-195F	140458

APC: allophycocyanin; CD: cluster of differentiation; FITC: fluorescein isothiocyanate; IgG: immunoglobulin G; PE: phycoerythrin.

Table S2. MIFlowCyt checklist.

Requirement	Please Include Requested Information
1.1. Purpose	To compare the concentrations of EVs released from activated platelets (CD61+/P-selectin+ or fibrinogen+), leukocytes (CD45+), ECs (CD31+/CD146+) and all procoagulant EVs (PS+) in PFP between 30 patients treated with ticagrelor and 30 patients treated with clopidogrel after first AMI.
1.2. Keywords	ADP receptors, extracellular vesicles, platelets, P2Y12 antagonists, ticagrelor
1.3. Experiment variables	Time after first AMI (24 hours, 72 hours, 6 months) and treatment (ticagrelor, clopidogrel) of patients
1.4. Organization name and address	Amsterdam University Medical Centers Location Academic Medical Centre Meibergdreef 9 1105 AZ Amsterdam The Netherlands
1.5. Primary contact name and email address	Aleksandra Gąsecka, a.gasecka@amc.uva.nl
1.6. Date or time period of experiment	July 2018– December 2018
1.7. Conclusions	EV concentrations increased over time after AMI. Compared to clopidogrel, ticagrelor attenuated the increase of EV concentrations over time after AMI.
1.8. Quality control measures	All samples were measured using an autosampler, which facilitates subsequent measurements of samples in a 96-well plate (see MIFlowCyt 1.9). Each well plate contained buffer-only controls (section S1.4), antibody in buffer controls (section S1.5), unstained controls (section S1.6) and isotype controls (section S1.7). The flow rate was cross calibrated with Rosetta Calibration (Exometry, Amsterdam, The Netherlands) and TruCount beads (BD Biosciences, Franklin Lakes, NJ, USA; section S1.9). Fluorescence detectors were calibrated (section S1.10) with 2 µm Q-APC beads (2327-51, BD), Quantum FITC-5 MESF beads

	(FCSC555A, Bio-Rad, Hercules, CA, USA), and SPHERO Easy Calibration Fluorescent Particles (EFCP-F2-5K, Spherotech Inc., Irma Lee Circle, IL, USA). FSC and SSC were calibrated with Rosetta Calibration (v1.11, section S1.11).
1.9 Other relevant experiment information	The entire study involved fifteen 96-well plates that were measured within 5 months during three periods of 7 subsequent days, 2 subsequent days and 1 day.
2.1.1.1. Sample description	Thawed platelet free plasma (PFP; MIFlowCyt 2.1.1.2) from hospitalized humans after first AMI (MIFlowCyt 2.1.1.3).
2.1.1.2. Biological sample source description	Blood collected in 10 mL 0.109 M citrated plastic tubes (S-Monovette, Sarstedt) via antecubital vein puncture using a 19-gauge needle, without tourniquet (the first 2 mL were discarded to avoid pre-activation of platelets). Within maximum 15 minutes from blood collection, platelet-depleted plasma was prepared by double centrifugation using a Rotina 380 R equipped with a swing-out rotor and a radius of 155 mm (Hettich Zentrifugen, Tuttlingen, Germany). The centrifugation parameters were: 2,500 g, 15 minutes, 20°C, acceleration speed 1, no brake. The first centrifugation step was done with 10 mL whole blood collection tubes. Supernatant was collected 10 mm above the buffy coat. The second centrifugation step was done with 3.5 mL plasma in 15 mL polypropylene centrifuge tubes (Greiner Bio-One B.V). Supernatant (platelet-depleted plasma) was collected 5 mm above the buffy coat, transferred into 5 mL polypropylene centrifuge tubes (Greiner Bio-One B.V), mixed by pipetting, transferred to 1.5 mL low-protein binding Eppendorfs (Thermo Fisher Scientific) and stored in -80°C. Before staining, samples were thawed for 1 minute at 37 °C.
2.1.1.3. Biological sample source organism description	Hospitalized humans after first AMI (for inclusion criteria, please see Table 1 of the manuscript).
2.2 Sample characteristics	Platelet free plasma (PFP) is expected to contain EVs, lipoproteins and proteins.

2.3. Sample treatment description	Please see section S1.3.
2.4. Fluorescence reagent(s) description	Please see Table S1.
3.1. Instrument manufacturer	Apogee, Hemel Hempstead, UK
3.2. Instrument model	A60-Micro
3.3. Instrument configuration and settings	Samples were analysed for 2 minutes at a flow rate of 3.01 $\mu\text{L}/\text{min}$ on an A60-Micro, equipped with a 405 nm laser (100 mW), 488 nm laser (100 mW) and 638 nm laser (75 mW). The trigger threshold was set at SSC 14 arbitrary units, corresponding to a side scattering cross section of 10 nm^2 (Rosetta Calibration). For FSC and SSC, the PMT voltages were 380 V and 360 V, respectively. For all detectors, the peak height was analysed. APC signals were collected with the 638-D Red(Peak) detector (long pass 652 nm filter, PMT voltage 510 V). FITC signals were collected with the 488-Green(Peak) detector (525/50 nm band pass filter, PMT voltage 520 V). PE signals were collected with the 488-Orange(Peak) detector (575/30 nm band pass filter, PMT voltage 520 V).
4.1. List-mode data files	A summary of all flow cytometry scatter plots and gates applied are available via https://www.doi.org/10.6084/m9.figshare.11340386 . Raw data and data with standard units (40 GB) will become available via SURFfilesender upon request (e.vanderpol@amsterdamumc.nl).
4.2. Compensation description	No compensation was required because no fluorophore combinations were used that have overlapping emission spectra.
4.3. Data transformation details	No data transforms were applied.
4.4.1. Gate description	To automatically apply gates, generate pdf reports with scatter plots, and summarize the data in a table, custom-build software (MATLAB R2018b) was used. Please find below a description of the gates.

	<p>First, only events that were collected during time intervals, for which the count rate was within 25% of the median count rate, were included.</p> <p>Second, residual platelets were excluded by applying a gate at the side scattering cross section ($<2,000 \text{ nm}^2$) and, depending on the fluorescence label, at a fluorescence channel (see compressed data summary files S2). For samples stained with CD61-APC, CD61-APC aggregates were omitted by selecting data fulfilling the condition stated by equation $\text{SSC}(\text{nm}^2) > \text{APC}(\text{MESF}) + 3$.</p> <p>Third, to include particles within the dynamic range of Flow-SR [3], particles with a diameter $>200 \text{ nm}$ and fulfilling the condition of equation S2 were included.</p> <p>Fourth, to exclude false positively labeled chylomicrons and thus primarily include EVs, only particles with a refractive index <1.42 were included.</p> <p>Fifth, fluorescence gates were automatically determined with a mathematical algorithm (MATLAB R2018b) and applied. Lower bounds of the fluorescent gates are 150 MESF for CD61-APC, 83 MESF for CD62p-PE, 550 MESF for fibrinogen-FITC, 91 MESF for CD45-APC, 101 MESF for CD31-APC, 85 MESF for CD146-PE, 590 MESF for lactadherin-FITC, and 123 MESF for CD235a-PE.</p>
4.4.2. Gate statistics	The number of positive events was corrected for flow rate, measurement time and dilutions performed during sample preparation.
4.4.3. Gate boundaries	<p>On overview of all gates can be found in the compressed data summary files</p> <p>(https://www.doi.org/10.6084/m9.figshare.11340386, CD31-APC_CD146-PE_gates.pdf, CD45-APC_Lac-FITC_gates.pdf, CD61-APC_CD62p-PE_gates.pdf, CD61-APC_Fib-FITC_gates.pdf, and CD235-PE_gates.pdf).</p>

ADP: adenosine diphosphate; AMI: acute myocardial infarction; ECs: endothelial cells; EVs: extracellular vesicles; FSC: forward scattering; PFP: platelet free plasma; PS: phosphatidylserine; SSC: side scattering.

Table S3: Additional orally administered pharmacotherapy at discharge and at 6 months.

Characteristic	Ticagrelor (n=27)		Clopidogrel (n=28)		p-value
	n	%	n	%	
Pharmacotherapy at discharge					
Allopurinol	2	7	1	4	ns
Calcium channel blocker	3	11	3	11	ns
Carbamazepine	0	0	1	4	ns
Diuretic	6	22	8	29	ns
Escitalopram	0	0	1	4	ns
Ezetymibe	1	4	1	4	ns
Metformin	3	11	3	11	ns
Pancreatine	0	0	1	4	ns
Potassium	8	30	9	32	ns
Sulfonylureas	1	4	2	7	ns
Tamsulosin	2	7	3	11	ns
Thyrosol	1	4	0	0	ns
Vitamin D	20	74	22	79	ns
α -tyroxin	2	7	1	4	ns
Pharmacotherapy at 6 months					
Allopurinol	1	4	1	4	ns
Calcium channel blocker	3	11	3	11	ns
Carbamazepine	0	0	1	4	ns
Diuretic	5	19	6	21	ns
Escitalopram	0	0	1	4	ns
Ezetymibe	1	4	1	4	ns
Metformin	3	11	4	14	ns
Pancreatine	0	0	1	4	ns
Potassium	6	22	7	25	ns
Sulfonylureas	1	4	2	7	ns
Tamsulosin	2	7	3	11	ns
Thyrosol	0	0	0	0	ns
Vitamin D	18	67	18	64	ns
α -tyroxin	2	7	1	4	ns